ACS APPLIED MATERIALS & INTERFACES

Research Article

www.acsami.org

Preparation of Chemically-Tailored Copolymer Membranes with Tunable Ion Transport Properties

Siyi Qu, Theodore Dilenschneider, and William A. Phillip*

Department of Chemical and Biomolecular Engineering, University of Notre Dame, Notre Dame, Indiana 46556-5637, United States

Supporting Information

ABSTRACT: Membranes derived from copolymer materials are a promising platform due to their straightforward fabrication and small yet tunable pore structures. However, most current applications of these membranes are limited to the size-selective filtration of solutes. In this study, to advance the utility of copolymer membranes beyond size-selective filtrations, a poly(acrylonitrile-*r*-oligo(ethylene glycol) methyl ether methacrylate-*r*-glycidyl methacrylate) (P(AN-*r*-OEGMA-*r*-GMA)) copolymer is used to fabricate membranes that can be chemically modified via straightforward schemes. The P(AN-*r*-OEGMA-*r*-GMA) copolymer is cast into asymmetric membranes using a nonsolvent induced phase separation technique. Then, the surface charge of the membrane is modified to tailor its performance for nanofiltration applications. The oxirane groups of the glycidyl methacrylate (GMA) moiety that line the pore walls of the membrane allows for both positively charged and negatively charged moieties to be introduced directly without any prior activation. Notably, the highly size-selective nanostructure of the copolymer materials is retained throughout the functionalization processes. Specifically, amine moieties are attached to the pore walls using the aminolysis of the oxirane groups. The resulting amine-functionalized membrane is positively charged and rejects up to 87% of the salt dissolved in a 10 mM magnesium chloride feed solution. Further modification of the amine-functionalized membrane with 4-sulfophenyl isothiocyanate results in pore walls lined by sulfonic acid moieties. These negatively charged membranes reject up to 90% of a 10 mM sodium sulfate feed solution. Throughout the modification scheme, the membrane permeability remains equal to 1.5 L m^{-2} h^{-1} bar^{-1} and the rejection of neutral solutes (i.e., sucrose and poly(ethylene oxide)) is consistent with the membrane having a single well-defined pore diameter of ~5 nm. The performance of the membrane as a function of ion valence number, solution pH, and ionic strength is investigated.

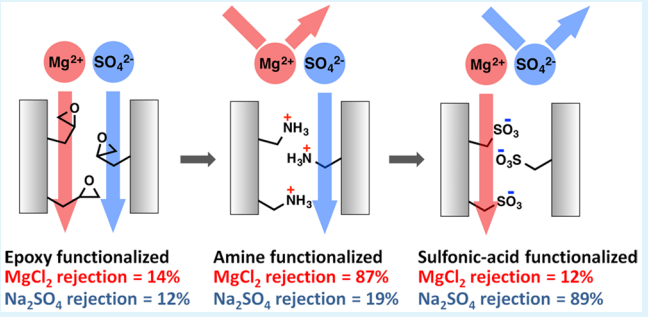

KEYWORDS: *nanofiltration, copolymer, glycidyl methacrylate, self-assembly, nonsolvent induced phase separation, ion permeation*

1. INTRODUCTION

Because of their small footprint, simple operation, and modular design, membrane devices are attractive options for a number of applications.[1−4] For example, membrane separations have been implemented successfully in desalination,[5−7] water treatment,[8−10] and pharmaceutical[11,12] processes. In these settings, the majority of the membranes implemented separate molecules using a size-selective mechanism. This reliance on steric hindrance or depth filtration mechanisms has limited the utility of membrane devices primarily to filtration and dialysis applications.[1,2,13,14] However, opportunities exist for the chemical functionalization of membranes to enhance the performance of some membrane processes by introducing new transport mechanisms or improving the lifetime of size-selective filters.[15−18] The development of straightforward and simple methods to alter the surface chemistry of membranes without damaging the nanostructures of the membranes is critical to the further advancement of processes that implement chemically tailored membranes.

Many techniques have been used to modify the pore chemistry of membranes including physical modifications, such as layer-by-layer assembly[19−21] and the deposition of nanomaterials,[22,23] and chemical modifications, such as coating with cross-linked hydrogels[24] and grafting polymer brushes to or from the membrane surface.[25−28] Significant progress has been made in optimizing these membrane modification schemes, but challenges remain. Physical modification techniques rely on van der Waals, hydrogen bonding, coordination, and electrostatic interactions to bind functional moieties to the surface of the membrane conformally. The ease and flexibility of these methods in addition to the fact that they do not disrupt the membrane structure are attractive features that have been used to make membrane adsorbers,[20,29] ion exchange membranes,[19,21] reactive membranes,[23] and gas-separation membranes.[30] However, when compared with chemical methods that covalently attach functional groups to the membrane surface, the lower stability of physically modified membranes during prolonged use or in extreme temperature or pH

Received: June 23, 2015
Accepted: August 19, 2015
Published: August 19, 2015

DOI: 10.1021/acsami.5b05592
ACS Appl. Mater. Interfaces 2015, 7, 19746−19754

conditions is a concern. Conversely, methods to incorporate functional groups through a covalent bond demonstrate high stability and functionality. However, in some cases, the treatments used to initiate the surface reactions can result in unwanted side reactions or damage to the membrane nanostructure that can impact membrane performance negatively, which is a concern for these chemical functionalization methods.[31−33] Therefore, the continued development of methods to tune chemical functionality without disrupting the nanostructure of the membranes is necessary.

Membranes derived from copolymer-based precursors are one attractive platform for addressing the challenges that face current modification schemes. In particular, the microphase separation of copolymers results in membranes that are easy to process and possess a high density of pores with a well-defined size.[15,34,35] Furthermore, by designing the chemistry and macromolecular architecture cleverly during the synthesis of the copolymer, the ultimate structure and functionality of the membranes can be engineered in a rational, systematic manner.

Prior work has demonstrated that membranes, which exhibit exemplary performance as size-selective filters, can be fabricated from ampihiphilic copolymers.[36,37] Poly(acrylonitrile-*r*-oligo(ethylene glycol) methyl ether methacrylate) (P(AN-*r*-OEGMA)) is one specific example where the microphase separation of the poly(ethylene oxide) (PEO) brush from the polyacrylonitrile (PAN) matrix templates a bicontinuous structure containing pores that act as precise nanoscale sieves.[37] On this basis, we expand the application of these novel nanofiltration membranes by incorporating glycidyl methacrylate (GMA) into the copolymer membrane precursor. Glycidyl methacrylate represents an attractive platform for modifying the chemical functionality as functional moieties can be immobilized through the nucleophilic ring-opening of the epoxide group.[38−40] Because of the regular nanostructure generated by the PEO brushes and simple modifications enabled by the GMA moieties, membranes fabricated from poly(acrylonitrile-*r*-oligo(ethylene glycol) methyl ether methacrylate-*r*-glycidyl methacrylate) (P(AN-*r*-OEGMA-*r*-GMA)) materials should allow for the formation of stable chemical functionality while maintaining the nanostructural integrity of the membranes.

In this work, we report the fabrication of asymmetric nanofiltration membranes from the ampiphilic copolymer P(AN-*r*-OEGMA-*r*-GMA) and demonstrate that the structure of this nanoporous thin film results in a sharp size-selective filtration of solutes. Subsequently, the ring opening of the GMA group with a diamine allowed for positively charged moieties to be introduced in the solid-state.[39] Further modification of the amine-functionalized membrane with an isothiocyanate produces membranes functionalized with negatively charged sulfonic acid groups.[41,42] Hydraulic permeability measurements and solute rejection test with neutral molecules confirm that these straightforward modification schemes do not impact the performance of the membranes as size-selective filters. Importantly, solute rejection experiments conducted with charged solutes indicate clearly that the ion transport properties are easily tailored using these methods. This combination of small pore sizes and tunable chemical functionality provided by the copolymer-based membranes holds much potential for further applications in the fields of water purification, sensing, and bioprocessing.

2. MATERIALS AND METHODS

2.1. Materials. All chemicals were purchased from Sigma-Aldrich unless otherwise noted. Acrylonitrile, poly(ethylene glycol) methyl ether methacrylate (M_n = 500 g mol^{-1}), and glycidyl methacrylate were purified by passing them through a basic alumina (VWR, West Chester, PA) column prior to use. A Millipore water purification system (Milli Q Advantage A10, Millipore Corporation, Bilerica, MA) provided deionized water (DI water), which was used in preparing solutions for permeability and solute rejection tests and for rinsing the test cell at the conclusion of an experiment. PAN-400 ultrafiltration flat sheet membranes, which were used for mechanical support, were purchased from Nanostone Water, Inc. (Oceanside, CA).

2.2. Polymer Synthesis and Characterization. *2.2.1. Synthesis of P(AN-r-OEGMA-r-GMA).* The poly(acrylonitrile-*r*-oligo(ethylene glycol) methyl ether methacrylate-*r*-glycidyl methacrylate) (P(AN-*r*-OEGMA-*r*-GMA)) copolymer was synthesized using a free radical polymerization mechanism. Four grams of acrylonitrile, 4.0 g of poly(ethylene glycol) methyl ether methacrylate, 2.0 g of glycidyl methacrylate, 0.5 mol % azobis(isobutyronitrile) (AIBN) relative to total amount of monomer, and a stir bar were added to a round-bottom flask containing 30 mL of dimethyl sulfoxide (DMSO). The flask was purged with nitrogen gas for 1 h before heating the system to 60 °C for 20 h. Then, the solution was cooled to room temperature, and the polymer was precipitated in diethyl ether. The polymer was redissolved in DMSO and precipitated in diethyl ether three more times to remove residual monomer. The final product was dried in a vacuum oven for 24 h.

2.2.2. Characterization of P(AN-r-OEGMA-r-GMA) Polymer. The ^{1}H nuclear magnetic resonance (^{1}H NMR) spectra of the P(AN-*r*-OEGMA-*r*-GMA) copolymer were measured with a Bruker Advance III HD400 spectrometer, using deuterated dimethyl sulfoxide (DMSO-d_6) as the solvent. The molecular weight of polymer was determined using a dimethylformamide (DMF) gel permeation chromatography (GPC) system including a Waters 515 HPLC pump, a Waters 2414 refractive index detector, three Polymer Standards Services (PSS) columns (GRAM, 10^4, 10^3, and 10^2 Å) with DMF at 55 °C as eluent, volumetric flow rate = 1.00 mL min^{-1}. Linear poly(methyl methacrylate) (PMMA) standards (Polymer Standards Service-USA, Inc., Amherst, MA) with molecular weights ranging from 730 g mol^{-1} to 1 010 000 g mol^{-1} were used for calibration.

2.3. Membrane Fabrication, Functionalization, and Characterization. *2.3.1. Membrane Fabrication Procedure.* Membranes were cast using a nonsolvent induced phase separation (NIPS) method.[2,15,43] In this method, an 18.5 wt % solution of P(AN-*r*-OEGMA-*r*-GMA) polymer was prepared by dissolving the polymer in DMSO. Prior to casting a membrane the solution was filtered through a 1 μm syringe filter and stirred slowly overnight to facilitate the release of dissolved gases. A small volume (∼1 mL) of the casting solution was pipetted onto a PAN-400 membrane, which was taped to a glass plate, and a doctor blade set to a gate height of 67 μm was used to draw down a uniform thin film of polymer solution. Solvent was allowed to evaporate from the film for 5 min before plunging the film into a nonsolvent (isopropyl alcohol) bath. The membrane was stored in a sealed isopropyl alcohol bath until further functionalization or transport tests were conducted.

2.3.2. Preparation of Amine-Functionalized Membranes. The ring opening reaction between 1,6-diaminohexane and the epoxide moiety of GMA was used to generate amine-functionalized membranes.[39] A membrane sample was submerged in a 2 M aqueous solution of the diamine. The volume of the solution was selected such that a 10× molar excess of diamine, relative to the epoxide moieties within the membrane, was present. The membranes were incubated in the diamine solution at room temperature for up to 3 h. The membranes were rinsed and stored in DI water after functionalization.

2.3.3. Preparation of Sulfonic-Acid-Functionalized Membranes. The reaction between an isothiocyanate and a primary amine was used to produce sulfonic-acid-functionalized membranes.[41,42] Specifically, an amine-functionalized membrane was submerged in a 0.06 M 4-

DOI: 10.1021/acsami.5b05592
ACS Appl. Mater. Interfaces 2015, 7, 19746−19754

sulfophenyl isothiocyanate (sodium salt form) in ethanol solution for up to 4 h. The solution temperature was maintained at 60 °C. The membrane was removed, washed with DI water, and stored in DI water after functionalization.

2.3.4. Nanostructual and Chemical Characterization of Polymeric Membranes. Attenuated total internal reflectance-Fourier transform infrared (ATR-FTIR) spectra of the P(AN-*r*-OEGMA-*r*-GMA) parent membrane, the amine-functionalized membrane, and the sulfonic-acid-functionalized membrane were acquired using a Jasco FT/IR-6300 spectrophotometer. Prior to analysis, the membranes were dried in a vacuum oven for 3 h. The ATR-FTIR spectra were collected over the range of wavenumbers from 4500−650 cm^{-1}. The microstructure of the membranes was characterized by scanning electron microscopy (SEM) using a Magellan 400 field emission scanning electron microscope. One cm × 1 cm sections of membrane were cut with a razor blade and allowed to air-dry for several minutes before being fixed onto a SEM sample holder (Ted Pella Inc., Redding, CA) with carbon tape. For cross-sectional imaging, the dried membranes were submerged in liquid nitrogen for at least 5 min then cracked in half. During this process, the nonwoven layer of the PAN400 membrane was removed before the cracked membrane was attached perpendicularly to a SEM sample holder. The samples were coated with 2 nm of iridium to prevent charging. Typically, micrographs were collected at an accelerating voltage of 5 kV and a working distance of 4 mm.

2.4. Stirred Cell Filtration Experiments. *2.4.1. Hydraulic Permeability Tests.* One inch diameter sections of the P(AN-*r*-OEGMA-*r*-GMA) membrane, the amine-functionalized membrane, and the sulfonic-acid-functionalized membrane were punched out using a circular hole punch and placed in a 10 mL Amicon 8010 stirred cell (Millipore) with the copolymer selective layer facing up. The cell was filled with 10 mL of solution and pressurized with nitrogen gas. The permeating solution was collected in 20 mL scintillation vials that rested on a balance. The steady-state water flux at each applied pressure was calculated by measuring the mass of the permeate as a function of time. The variation of the water flux over a range of applied pressures from 20 to 60 psi was used to calculate the hydraulic permeability of the membranes.

2.4.2. Molecular Weight Cutoff Tests and Analysis. One gram per liter poly(ethylene oxide) (PEO) solutions were prepared by dissolving PEO samples of known molecular weights (1.1, 2.1, 4.0, 7.8, 10, and 35 kDa) in DI water to produce seven solutions. The PEO samples used for the molecular weight cutoff test were purchased from Polymer Source Inc. (Montreal, Quebec, Canada), and all had a dispersity ($Đ$) value less than 1.1. A 1 g L^{-1} sucrose solution was made by dissolving sucrose in DI water. The membranes were challenged with the sucrose solution and each PEO solution separately while stirring the solution at 600 rpm. The first 1 g of permeate was discarded and then two 1 g samples were collected in clean 20 mL scintillation vials. The vials were sealed and stored in a fridge until they were analyzed. During these experiments, the feed solutions were continuously refilled to maintain at least 8 mL in the stirred cell. The stir cell was emptied and rinsed with DI water at least 3 times between each test. The concentrations of PEO in the permeate and feed solutions collected during each experiment were measured with a Shimadzu TOC-TN Organic Carbon Analyzer. The percent rejection was calculated according to the equation

$$R\ (\%) = \left(1 - \frac{C_p}{C_f}\right) \times 100 \qquad (1)$$

where C_p and C_f represent the concentrations of PEO in the permeate and the feed, respectively.

2.4.3. Salt Retention Tests and Analysis. Single salt solutions of sodium chloride (NaCl), magnesium chloride ($MgCl_2$), sodium sulfate (Na_2SO_4), and magnesium sulfate ($MgSO_4$) were prepared by dissolving each salt in DI water at the prescribed concentration. Salt rejection was determined by filling the stirred cell with a salt solution and driving permeation using N_2 gas. The permeate was collected in clean 20 mL scintillation vials. The feed solutions were continuously refilled to maintain at least 8 mL. Between experiments with the same salt at different concentrations or different salts, the stir cell was emptied and rinsed with DI water at least 3 times and 1 g of DI water was passed through membrane.

The concentrations of magnesium chloride and magnesium sulfate in the permeate and feed solution samples were measured using a PerkinElmer Optima 8000 Inductively Coupled Plasma Optically Emitting Spectra (ICP-OES) to quantify the concentration of Mg^{2+}. The concentrations of sodium chloride and sodium sulfate in the permeate and feed solution samples were measure using a Dionex ICS-5000 ion chromatography (IC) system to quantify the concentration of Na^+, Cl^-, and SO_4^{2-}. The percent rejection for the various salts was calculated using eq 1.

2.4.4. pH Dependent Transport Properties. Some tests required the solution to be adjusted to a specific pH. A 50 mL sample of the solution was placed into a beaker, and hydrochloric acid or sodium hydroxide was added as needed to adjust the pH between 2.5 and 11. Values of the pH were measured using an Accumet AP115 portable pH meter (Fisher Scientific, Waltham, MA). Before the sample was used in an experiment, the beaker was sealed using Parafilm until the pH reading was stable. Transferring the sample to the stirred cell was done quickly to minimize exposure to the open atmosphere.

3. RESULTS AND DISCUSSIONS

3.1. Copolymer Synthesis and Characterization. The P(AN-*r*-OEGMA-*r*-GMA) copolymer was synthesized using a free radical polymerization mechanism. This particular copolymer was used because the PAN allows for the formation of a robust, mechanically stable matrix, the PEO side chains of the poly(oligo(ethylene glycol) methyl ether methacrylate) (POEGMA) microphase separate from the matrix to produce a continuous network of water permeable pores,[37,44] and the GMA functionality allows for the pore walls of the membranes to have specific and easily tailored functionality.

A combination of ^{1}H NMR spectroscopy and gel permeation chromatography (GPC) indicated the synthesis of a high molecular weight copolymer that contained AN, OEGMA, and GMA moieties. GPC analysis, based on PMMA standards, indicated that the average molecular weight of the material was 250 kg mol^{-1} with a dispersity ($Đ$) value of 3.2 (Figure S1). The weight fractions of AN, OEGMA, and GMA in the copolymer material, as determined by ^{1}H NMR, were 40%, 40%, and 20%, respectively (Figure 1). PEO weight content was calculated from ratio of side chain PEO protons (3.5 ppm) to total backbone tail protons (1.7−2.2 ppm), which was equal to 32%.

In addition to a sufficient fraction of PEO to produce a continuous network of pores that percolated through the membrane, microphase separation of the PEO side chains from the matrix-forming material is critical to the generation of permeable membranes.[37] Differential scanning calorimetry (DSC) was used to characterize the thermal transitions of the P(AN-*r*-OEGMA-*r*-GMA) copolymer (Figure S2). A glass transition was observed around −55 °C, which is consistent with the glass transition temperature of noncrystalline PEO homopolymer.[45] Another glass transition, which can be attributed to the backbone rotation of the PAN matrix, was observed at 145 °C.[46] The presence of two distinct glass transition temperatures is consistent with microphase separation of the P(AN-*r*-OEGMA) material.[37,44] As such, the GMA moieties that enable the straightforward functionalization of the membrane pores in the solid-state should not interfere with the fabrication of size-selective membranes.

3.2. Epoxy-Functionalized Membranes. *3.2.1. Membrane Fabrication.* Asymmetric membranes were prepared

DOI: 10.1021/acsami.5b05592
ACS Appl. Mater. Interfaces 2015, 7, 19746−19754

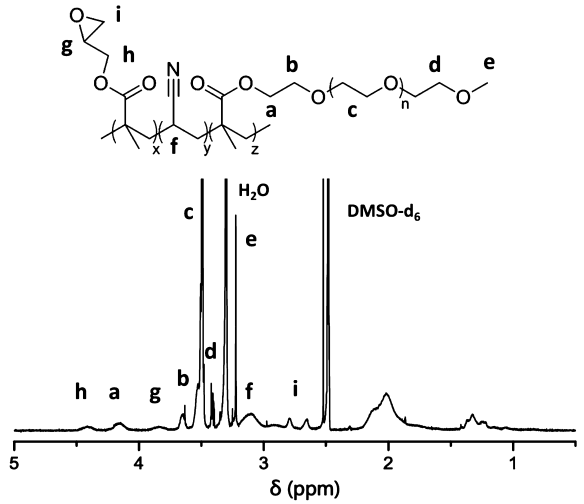

Figure 1. ^{1}H NMR spectra of P(AN-*r*-OEGMA-*r*-GMA) copolymer. Characteristic peaks and corresponding protons from each moiety are labeled. The a and b, f, and h peaks are used to determine the relative composition of OEGMA, AN, and GMA, respectively, in the copolymer.

from the P(AN-*r*-OEGMA-*r*-GMA) copolymer using the NIPS method as described above. Cross sectional micrographs of the membranes, which show a thin active layer on top of a thicker support layer, are displayed in Figure S3. When solvent is allowed to evaporate from the coated film of casting solution, the polymer density increases at the film−air interface. This facilitates the microphase separation of the PEO side chains and matrix forming polymer, which templates the bicontinuous structure that makes these membranes highly selective nanofilters. The underlying support layer, which possesses more porous macrovoids, is formed during the nonsolvent induced precipitation step.[47,48]

3.2.2. Membrane Characterization. Transport tests, specifically hydraulic permeability and solute rejection experiments, were conducted using the epoxy-functionalized membrane prior to chemical modification to demonstrate its performance as a size-selective filter. Using a stirred cell, the hydraulic permeability of the membranes was determined by measuring the water flux at applied pressures that ranged from 20 to 60 psi (Figure 2a). The hydraulic permeability of the epoxy-functionalized membranes was 1.5 ± 0.7 L m^{-2} h^{-1} bar^{-1}.

In addition to the hydraulic permeability, the ability of the P(AN-*r*-OEGMA-*r*-GMA) membrane to filter dissolved solutes based on size was quantified. For these experiments, the membrane was challenged with solutions containing sucrose or poly(ethylene oxide) (PEO) molecules that varied in molecular weight from 1.1 to 35 kDa. The hydrodynamic diameters of the PEO samples were calculated using literature data for the intrinsic viscosity and diffusion coefficients of PEO in aqueous solutions. Based on these correlations, the hydrodynamic diameters were determined to range from 1.7 to 11.7 nm.[49,50] Sucrose has a well-characterized hydrodynamic diameter of 1.06 nm.[51] The percent rejection eq 1 is plotted as a function of the hydrodynamic diameter in Figure 2b. The higher molecular weight samples (4.0−35.0 kDa) are almost completely rejected (Figure S4). In contrast, the 1.1 kDa and 2.1 kDa PEO and sucrose samples are only rejected partially. The rapid decline in rejection for samples with molecular weights less than 4.0 kDa indicates a narrow pore size distribution with an average pore

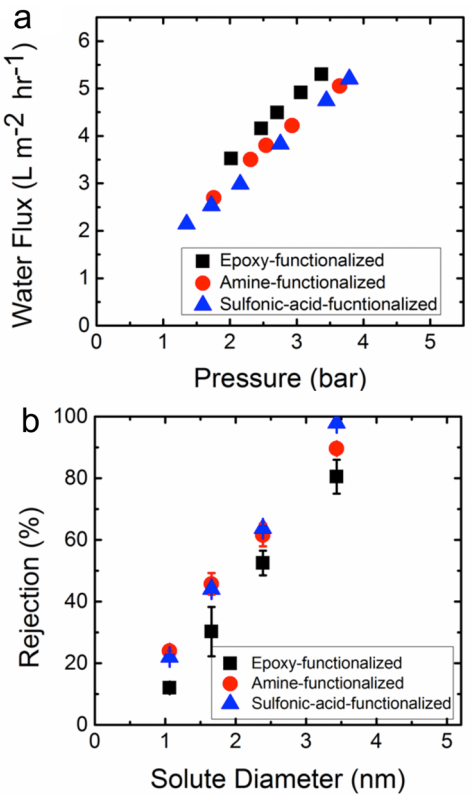

Figure 2. (a) DI water flux vs applied pressure for the epoxy-functionalized, amine-functionalized and sulfonic-acid-functionalized copolymer membranes. The hydraulic permeabilities of the membranes were determined from the slope of the data, which were generated by measuring water flux at applied pressures ranging from 20 to 60 psi. (b) Solute rejection curves for the epoxy-functionalized, amine-functionalized and sulfonic-acid-functionalized copolymer membranes. Sucrose and poly(ethylene oxide) (PEO) molecules of known size were used as neutral solutes. Feed solutions were made by dissolving sucrose (342 g mol^{-1}) or PEO samples with molecular weights of 1.1, 2.1, and 4.0 kg mol^{-1} in DI water. The percent rejection was determined by taking the ratio of the sucrose or PEO concentration in the permeate to the 1 g L^{-1} feed. Error bars indicate one standard deviation in measurements from multiple experiments.

size similar to that of the 4.0 kDa molecules. Because of their neutral charge and minimal interactions with the surrounding environment, we assumed that the sucrose and PEO molecules were being sieved from solution based solely on size. This assumption allowed us to estimate the characteristic pore size of the epoxy-functionalized membrane using the theory for hindered transport proposed by Zeman and Wales.[14] In particular, the rejections of sucrose, the 1.1 kDa (1.7 nm) and 2.1 kDa (2.4 nm) PEO samples, 12%, 30%, and 52%, respectively, are consistent with an average pore size of 5.6 nm.

3.3. Preparation of Charge-Functionalized Membranes. *3.3.1. Membrane Functionalization Protocols.* The unique nanostructure of the P(AN-*r*-OEGMA-*r*-GMA) copolymer membrane results in a sharp molecular weight cutoff that makes the membrane well-suited for size selective filtrations. In many applications of membrane devices, it is desirable to tailor the interactions between the membrane and the surrounding solution. However, as noted previously, many of the membrane functionalization schemes reported to date lead to undesired changes in the pore structure of the parent membrane. This complicates the systematic design of the membrane structure

DOI: 10.1021/acsami.5b05592
ACS Appl. Mater. Interfaces 2015, 7, 19746−19754

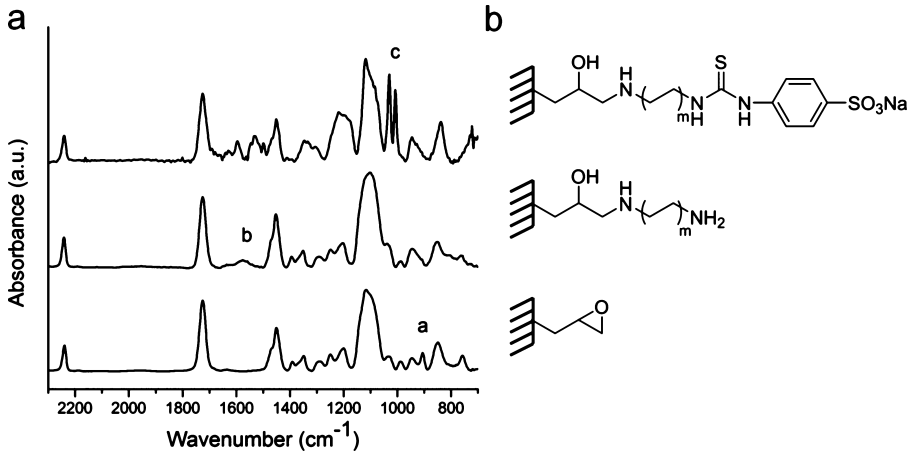

Figure 3. ATR-FTIR spectra of the functional copolymer membranes. In the lower spectrum, for a native P(AN-*r*-OEGMA-*r*-GMA) membrane, the signal at ∼908 cm^{-1} corresponds to the antisymmetric ring deformation band of the epoxide group in GMA labeled a. In the middle spectrum, for a P(AN-*r*-OEGMA-*r*-GMA) membrane immersed in a 2 M aqueous solution of 1,6-diaminohexane for 3 h, the intensity of the epoxide peak decreases. The intensity of the signal at ∼1580 cm^{-1}, which corresponds to N−H bending band labeled b, increases. In the top spectrum, for an amine-functionalized membrane reacted with 4-sulfophenyl isothiocyanate sodium salt monohydrate for 4 h, the intensity of the signals at ∼1033 cm^{-1}, which corresponds to the sulfonic acid group vibrational adsorption peaks labeled c. The spectra are normalized with respect to carbonyl stretch band at ∼1725 cm^{-1}.

and chemistry. Here, the incorporation of the GMA moiety prior to membrane fabrication enables the facile modification of the chemistry that lines the pore walls in the solid-state (i.e., after fabrication). In this study, the nucleophilic oxirane ring-opening reaction is used to systematically modify the chemistry within the pores with relative ease. Specifically, the ring-opening reaction with a diamine was investigated to produce a membrane with amine groups lining the pore walls. By incubating the membrane in diamine solution, the epoxide groups reacted with one amino-group, immobilizing the other amino-group inside the pore. At predefined reaction times, the substrates were taken out from the reaction solutions, thoroughly rinsed with water, and air-dried. These samples were analyzed by FTIR. A time series of the FTIR spectra is included in the Supporting Information as Figure S5. Based on these data, the reaction was complete after 90 min. The terminal spectrum is displayed in Figure 3 along with the spectra of the parent epoxy-functionalized membrane. Between the bottom and middle spectra in Figure 3, the epoxide signal at 908 cm^{-1} disappears, which is good evidence for the ring-opening of the oxirane group.[38] The successful aminolysis of the side chains is further evidenced by the appearance of N−H bending band around 1580 cm^{-1}. This suggests that the epoxy-functionalized membrane is modified into amine-functionalized membrane, which should possess a positive charge when the amine groups protonate.

The amine groups also can serve as new active sites for further chemical modification. Here, the amine-functionalized membrane was reacted with sulfophenyl isothiocyanate sodium salt in ethanol solution at 60 °C. A time series of the FTIR spectra is included in the Supporting Information (Figure S5), with the terminal spectrum included at the top of Figure 3. The terminal spectrum shows an intense peak at ∼1033 cm^{-1},[52] which is characteristic of sulfonic acid group vibration. This indicates that sulfonic acid groups replaced the amine groups inside the nanochannels after the reaction between the isothiocyanate and amine. Consequently, the resulting sulfonic-acid-functionalized membranes should possess a negative charge at most pHs because of the covalently attached sulfonic acid group. In this way, after two straightforward solid states modifications, the functional groups lining the pore wall of the copolymer membrane changed from oxirane to amine to sulfonic acid, and a corresponding change in the membrane surface charge from neutral to positive to negative should also be observed with little change to the membrane structure.

The fabricated terpolymer membrane and the postmodified membranes were characterized using both microscopy and transport tests. Scanning electron microscopy reveals a smooth, defect-free surface of the copolymer membrane both before and after modification reactions (Figure S6) suggesting that there is no significant damage to the membrane structure caused by the functionalization with amine or sulfonic acid groups. Moreover, transport tests support the assertion that the self-assembled structure of the membrane remains intact after the functionalization reactions. The hydraulic permeability of the membrane after each modification step was 1.5 ± 0.7 L m^{-2} h^{-1} bar^{-1}(Figure 2a), which is consistent with the permeability of the epoxy-functionalized membrane. The solute rejection curves for the amine-functionalized membrane and sulfonic-acid functionalized membrane are compared with the rejection curve for the epoxy-functionalized membrane in Figure 2b. PEO rejection decreases sharply around a PEO molecular weight of 4 kDa, which is in good agreement with the original epoxy-functionalized membrane. The combined results from water flow and solute rejection tests provide solid evidence that the membrane nanostructure remains intact after the functionalization process.

3.3.2. Tunable Ion Permeation Properties of Charge Functionalized Membranes. The membrane nanostructure, and ability to perform as a highly size-selective filter, remains intact after each step of the functionalization process. However, the incorporation of amine and sulfonic acid moieties will affect the interactions between the membrane and solutes in solution. For example, the positively charged amine and negatively charged sulfonic acid groups can enhance the rejection of charged solutes. Co-ions (i.e., those with the same charge as the membrane) will be repelled by the charged membrane surface, and the counterions (i.e., those with the opposite charge as the

DOI: 10.1021/acsami.5b05592
ACS Appl. Mater. Interfaces 2015, 7, 19746−19754

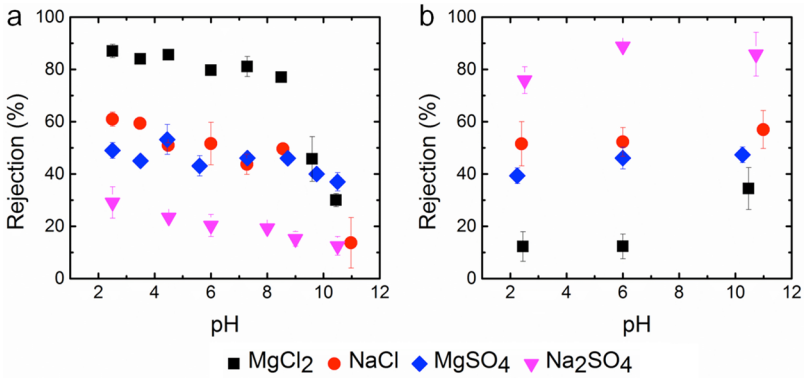

Figure 4. Salt rejection as a function of pH for amine-functionalized membrane (a) and sulfonic-acid-functionalized membrane (b). The percent rejection was determined by taking the ratio of the ion concentration in the permeate to the 10 mM feed. For solutions containing $MgCl_2$ or $MgSO_4$, the Mg^{2+} concentration was determined using ICP-OES. For the solutions containing NaCl or Na_2SO_4, percent rejection was calculated using the anion and cation concentrations determined by IC. The salts were dissolved in DI water and the pH was adjusted by adding HCl, HNO_3, or NaOH as needed. An applied pressure of 50 psi was used to drive permeation in all of the experiments. Error bars indicate one standard deviation in measurements from multiple experiments.

membrane) will be retained near the membrane due to the energy penalty associated with charge separation.[53,54] The balance between these effects is critical to the ability of the membrane to remove dissolved salts from solution.

The solute rejection experiments using PEO suggested that the membranes possess an active layer with a consistent, well-defined pore size around 5 nm. In comparison, the hydrodynamic diameters of dissolved ions typically range from 0.60 to 0.86 nm.[55] As such, the steric hindrance of ions by the membrane should not be significant, and the ions should permeate freely.[56,57] Salt rejection experiments conducted with a 10 mM $MgCl_2$ solution and the epoxide-functionalized membrane confirmed this hypothesis. The neutral membrane rejected only 14% of the $MgCl_2$. For the charge-functionalized membranes, however, electrostatic interactions will affect ion rejection greatly. The Donnan theory for membrane equilibria gives an idealized framework for examining the retention of point-charge ions by a charged membrane.[58] In particular, it predicts that charged membranes will exhibit higher rejection of salts with multivalent co-ions and monovalent counterions and a lower rejection of salts having multivalent counterions and monovalent co-ions.[56]

Solute rejection experiments were conducted using 10 mM feed solutions of $MgCl_2$, $MgSO_4$, Na_2SO_4, NaCl at pH 6.0 to investigate the role electrostatic interactions play in the performance of charge-functionalized copolymer membranes. The percent rejection of each electrolyte by the positively charged amine-functionalized membrane are compared in Figure 4a. At pH 6.0, the salt rejection results follow a sequence of $R(MgCl_2) = 81\% > R(NaCl) = 52\% \approx R(MgSO_4) = 43\% > R(Na_2SO_4) = 20\%$, which is consistent with the Donnan theory.[56,58,59] For the sulfonic-acid-functionalized membrane with negatively charged pore walls, the sequence of salt rejection at pH 6.0 is switched. In this case, $R(MgCl_2) = 12\% < R(NaCl) = 52\% \approx R(MgSO_4) = 46\% < R(Na_2SO_4) = 89\%$ as shown in Figure 4b. Because the membrane charge switches after covalently binding the sulfonic acid moiety within the pores, the reversal of the rejection sequence is consistent with the Donnan theory. Given the results above, which demonstrate that the charge state of the terminal groups within the pores determine the trend in ion rejection, we conclude that the membranes have been functionalized successfully.

3.4. Influence of Solution Properties on the Performance of Charge-Functionalized Membranes. *3.4.1. Solution pH.* The results above demonstrate the significant role electrostatic interactions play in the ability of the charge-functionalized membranes to mediate the transport of electrolytes. Therefore, the rejection of ionic solutes is expected to depend on the properties of the feed solution including ionic strength and the values of the solution pH. To probe the influence of solution pH on membrane performance, salt rejection was measured over a range of acidic and basic conditions between pH 2.5 and pH 10.5.

The surface charge of the functionalized membranes is determined by the state of the terminal functional group. In the case of the sulfonic-acid-functionalized membrane, the terminal sulfonate group imparts negative surface charge to the membrane. Because the sulfonate groups are a strong acid ($pK_a = -0.6$),[60] they remained deprotonated, and negatively charged, over the whole pH range evaluated. As such, the charge density of the membrane did not undergo a dramatic change, and a constant value for percent rejection is observed for each ion in Figure 4b. A slight uptick in percent rejection was observed for $MgSO_4$ at pH 10.5, which is likely the result of its low solubility at this pH causing some precipitation. The precipitate would be filtered readily based on their relatively large size.

The terminal amine groups determine the surface charge of the amine-functionalized membrane. Unlike the sulfonic acid moieties, the amine moieties are weak electrolytes so their charge depends on the solution pH. Below the pK_a of the amine ($pK_a = 10.7$),[60] the membrane is positively charged due to the protonation of the amine groups bound to the pore walls. This created a high density of positive charge that resulted in the effective rejection of cations from solutions at a pH below 9. As the pH increases, the amine groups deprotonate reducing the charge density of the membrane. Eventually, above the pK_a of the amine moieties, the membrane possessed essentially no charge. Figure 4a demonstrates the effect of amine protonation/deprotonation on membrane performance. Around a pH value of 10, the rejection of all the salts decreased sharply. The effect is most notable for $MgCl_2$ whose percent rejection fell from 87% to around 30%.

Often, the protonation and deprotonation of weak electrolytes fixed to a pore wall result in structural rearrangements that

DOI: 10.1021/acsami.5b05592
ACS Appl. Mater. Interfaces 2015, 7, 19746−19754

reduce the effective pore size of the membrane and decrease permeability.[15,21,61] Water flux and solute rejection experiments were conducted over the same range of solution pH as the salt rejection experiments to explore the possibility of structural rearrangements causing the observed salt rejections. Only the amine-functionalized membrane was used in these experiments because the sulfonic acid membrane did not demonstrate a pH dependent salt rejection. The results of these experiments are presented in Figure 5. Over a range of solution pH from pH 2.5

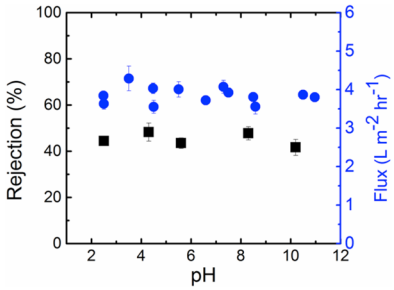

Figure 5. Solution flux (10 mM NaCl DI water solution, applied pressure 50 psi) and percent rejection of 1.1 kDa poly(ethylene oxide) (PEO) molecules as a function of pH for hexamethylenediamine functionalized membrane. Both salt and PEO are dissolved in DI water and pH altered by the addition of aqueous HCl and NaOH solutions, as needed. Error bars indicate one standard deviation in measurements from multiple experiments.

to pH 10.5, there was no significant change in the permeability of the membrane. In conjunction with the constant rejection value of the 1.1 kDa PEO molecule, which is neutral, over the same pH range, this data precludes the possibility of the solution pH inducing structural changes. Prior studies have demonstrated that dissolved cations at concentrations above 0.3 M can have a significant effect on the conformation of PEO molecules. However, the low concentration of acid and base used here to adjust the solution pH (~1 to 10 mM) should not affect the conformation, and therefore hydrodynamic size, of the dissolved PEO molecules.[62] In conclusion, the combined results demonstrating tunable electrostatic interactions and constant steric hindrance over a range of solution pH provide a strong argument that the pore structure is retained and salt retention is dominated by the charge of the membrane.

3.4.2. Ionic Strength. Because electrostatic interactions between the charged membranes and dissolved ions play a significant role in ion rejection, ion rejection should be sensitive to solution ionic strength. Figure 6 shows $MgCl_2$ rejection as a function of feed solution concentration for the amine-functionalized membrane. The feed solution was at pH 2.0. For feed solutions at low concentrations (0.5 mM, 1 mM), $MgCl_2$ rejection is as high as 96%. Rejection decreases slightly to 87% for a feed concentration of 10 mM $MgCl_2$. However, when the ion concentration was increased to 100 mM, the rejection of Mg^{2+} ions dropped significantly to a value of 36%. These results suggest that ion rejection is almost complete and independent of the ionic strength of the feed solution as long as the Debye length is greater than the pore radius (2.3 nm). The Debye lengths for the 0.5 mM, 1 mM and 10 mM $MgCl_2$ feed solutions are 7.9, 5.6, and 1.8 nm, respectively.[63] At a feed concentration of 100 mM, the Debye length decreases to 0.56 nm, which is a small fraction of the pore radius and as a result ion rejection decreases. A similar dependence on ionic strength

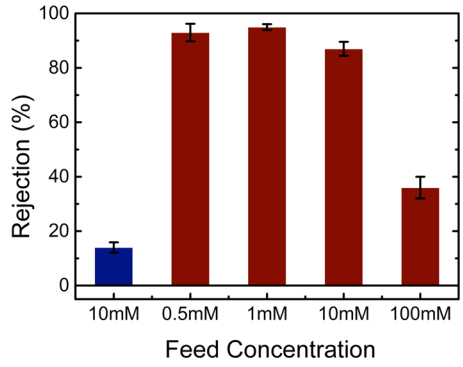

Figure 6. Ion rejection as a function of the concentration of $MgCl_2$ in the feed solution. for the hexamethylenediamine functionalized membrane and the parent P(AN-*r*-OEGMA-*r*-GMA) membrane rejection of 10 mM $MgCl_2$ solution. The percent rejection was determined by taking the ratio of the salt concentration in the permeate to the 10 mM feed. The concentrations of magnesium ions in the feed and permeate solutions were measured with ICP-OES. The $MgCl_2$ was dissolved in DI water, and the pH of the solution was adjusted to 2.5 by adding HCl. An applied pressure of 50 psi was used in the experiments. Error bars indicate one standard deviation in measurements from multiple experiments.

was found in prior work on charged carbon nanotube membranes.[54]

4. CONCLUSIONS

The results presented above demonstrate the use of the amphiphilic copolymer P(AN-*r*-OEGMA-*r*-GMA) to fabricate size-selective filters that can be chemically tailored. The microphase separation of the PEO side chains produces membranes with a well-defined pore size of ~5 nm. The high density of oxirane groups distributed throughout the pores of the membrane allowed straightforward and rapid modification schemes to be used to tailor the surface charge of the membrane. The introduction of charged moieties has a strong effect on the ability of the P(AN-*r*-OEGMA-*r*-GMA) to reject dissolved salts, but does not affect the permeability of the membrane or its ability to selectively filter neutral solutes. As such, the independent control over structure and chemical functionality provided by the P(AN-*r*-OEGMA-*r*-GMA) membrane platform will allow for the membrane properties to be tuned for a number of specifically targeted separations and nanoscale applications.

■ ASSOCIATED CONTENT

Supporting Information

The Supporting Information is available free of charge on the ACS Publications website at DOI: 10.1021/acsami.5b05592.

GPC trace of the P(AN-*r*-OEGMA-*r*-GMA) copolymer, DSC trace of the P(AN-*r*-OEGMA-*r*-GMA) copolymer, cross-sectional SEM micrographs of the PAN400 membrane used as a support and the copolymer composite membrane, ATR-FTIR spectra monitoring the P(AN-*r*-OEGMA-*r*-GMA) membrane functionalization reactions as a function of time, SEM micrographs of epoxy-functionalized, amine-functionalized, and sulfonic-acid-functionalized membrane surface (PDF)

DOI: 10.1021/acsami.5b05592
ACS Appl. Mater. Interfaces 2015, 7, 19746−19754

AUTHOR INFORMATION

Corresponding Author

*E-mail: wphillip@nd.edu.

Author Contributions

The manuscript was written through contributions of all authors. All authors have given approval to the final version of the manuscript.

Notes

The authors declare no competing financial interest.

ACKNOWLEDGMENTS

Portions of this work were made possible with support from the Army Research Office (ARO) through the Polymer Chemistry Program (Award Number W911NF-14-1-0229, Program Manager Dr. Dawanne Poree) and we appreciatively acknowledge this support. W.A.P. gratefully acknowledges support from the 3M Non-Tenured Faculty Award. We would like to thank Dr. Yi Shi for helpful discussions and assistance with the GPC measurements and Prof. Haifeng Gao in the Chemistry Department at the University of Notre Dame, the Notre Dame Integrated Imaging Facility (NDIIF), and the Center for Environmental Science and Technology (CEST) at Notre Dame; portions of this research were performed with instruments at these facilities.

REFERENCES

(1) Baker, R. W. *Membrane Technology and Applications*, 2nd ed.; J. Wiley: Chichester, U.K., 2004.

(2) Zhang, Y.; Sargent, J. L.; Boudouris, B. W.; Phillip, W. A. Nanoporous Membranes Generated from Self-assembled Block Polymer Precursors: Quo Vadis? *J. Appl. Polym. Sci.* **2015**, *132* (21), 41683−41699.

(3) Jackson, E. A.; Hillmyer, M. A. Nanoporous Membranes Derived from Block Copolymers: From Drug Delivery to Water Filtration. *ACS Nano* **2010**, *4* (7), 3548−3553.

(4) Adiga, S. P.; Jin, C.; Curtiss, L. A.; Monteiro-Riviere, N. A.; Narayan, R. J. Nanoporous Membranes for Medical and Biological Applications. *Wiley Interdiscip. Rev.: Nanomed. Nanobiotechnol.* **2009**, *1* (5), 568−581.

(5) Lorain, O.; Hersant, B.; Persin, F.; Grasmick, A.; Brunard, N.; Espenan, J. M. Ultrafiltration Membrane Pre-treatment Benefits for Reverse Osmosis Process in Seawater Desalting. Quantification in Terms of Capital Investment Cost and Operating Cost Reduction. *Desalination* **2007**, *203* (1), 277−285.

(6) Yun, T. I.; Gabelich, C. J.; Cox, M. R.; Mofidi, A. A.; Lesan, R. Reducing Costs for Large-scale Desalting Plants Using Large-Diameter, Reverse Osmosis Membranes. *Desalination* **2006**, *189* (1), 141−154.

(7) Elimelech, M.; Phillip, W. A. The Future of Seawater Desalination: Energy, Technology, and the Environment. *Science* **2011**, *333* (6043), 712−717.

(8) Geise, G. M.; Lee, H. S.; Miller, D. J.; Freeman, B. D.; McGrath, J. E.; Paul, D. R. Water Purification by Membranes: The Role of Polymer Science. *J. Polym. Sci., Part B: Polym. Phys.* **2010**, *48* (15), 1685−1718.

(9) Lewis, S. R.; Datta, S.; Gui, M. H.; Coker, E. L.; Huggins, F. E.; Daunert, S.; Bachas, L.; Bhattacharyya, D. Reactive Nanostructured Membranes for Water Purification. *Proc. Natl. Acad. Sci. U. S. A.* **2011**, *108* (21), 8577−8582.

(10) Shannon, M. A.; Bohn, P. W.; Elimelech, M.; Georgiadis, J. G.; Marinas, B. J.; Mayes, A. M. Science and Technology for Water Purification in the Coming Decades. *Nature* **2008**, *452* (7185), 301−310.

(11) Christy, C.; Vermant, S. The State-of-the-Art of Filtration in Recovery Processes for Biopharmaceutical Production. *Desalination* **2002**, *147* (1), 1−4.

(12) van Reis, R.; Zydney, A. Bioprocess Membrane Technology. *J. Membr. Sci.* **2007**, *297* (1), 16−50.

(13) Ho, W. W.; Sirkar, K. K. *Membrane Handbook*; Van Nostrand Reinhold: New York, 1992.

(14) Zeman, L.; Wales, M. Steric Rejection of Polymeric Solutes by Membranes with Uniform Pore Size Distribution. *Sep. Sci. Technol.* **1981**, *16* (3), 275−290.

(15) Mulvenna, R. A.; Weidman, J. L.; Jing, B.; Pople, J. A.; Zhu, Y.; Boudouris, B. W.; Phillip, W. A. Tunable Nanoporous Membranes with Chemically-Tailored Pore Walls from Triblock Polymer Templates. *J. Membr. Sci.* **2014**, *470*, 246−256.

(16) Rajesh, S.; Yan, Y.; Chang, H. C.; Gao, H. F.; Phillip, W. A. Mixed Mosaic Membranes Prepared by Layer-by-Layer Assembly for Ionic Separations. *ACS Nano* **2014**, *8* (12), 12338−12345.

(17) Asatekin, A.; Gleason, K. K. Polymeric Nanopore Membranes for Hydrophobicity-Based Separations by Conformal Initiated Chemical Vapor Deposition. *Nano Lett.* **2010**, *11* (2), 677−686.

(18) Rana, D.; Matsuura, T. Surface Modifications for Antifouling Membranes. *Chem. Rev.* **2010**, *110* (4), 2448−2471.

(19) Cheng, C.; White, N.; Shi, H.; Robson, M.; Bruening, M. L. Cation Separations in Electrodialysis Through Membranes Coated with Polyelectrolyte Multilayers. *Polymer* **2014**, *55* (6), 1397−1403.

(20) Jiang, Y.; Wang, W. C. Functional Membranes Prepared by Layer-by-Layer Assembly and its Metal Ions Adsorption Property. *Polym. Adv. Technol.* **2011**, *22* (12), 2509−2516.

(21) Armstrong, J. A.; Bernal, E. E. L. n.; Yaroshchuk, A.; Bruening, M. L. Separation of Ions Using Polyelectrolyte-Modified Nanoporous Track-Etched Membranes. *Langmuir* **2013**, *29* (32), 10287−10296.

(22) Barry, E.; McBride, S. P.; Jaeger, H. M.; Lin, X.-M. Ion Transport Controlled by Nanoparticle-Functionalized Membranes. *Nat. Commun.* **2014**, *5*, 5847−5854.

(23) Hilke, R.; Pradeep, N.; Madhavan, P.; Vainio, U.; Behzad, A. R.; Sougrat, R.; Nunes, S. P.; Peinemann, K.-V. Block Copolymer Hollow Fiber Membranes with Catalytic Activity and pH-Response. *ACS Appl. Mater. Interfaces* **2013**, *5* (15), 7001−7006.

(24) Ishihara, K.; Ueda, T.; Nakabayashi, N. Preparation of Phospholipid Polymers and their Properties as Polymer Hydrogel Membranes. *Polym. J.* **1990**, *22* (5), 355−360.

(25) Chu, L.-Y.; Li, Y.; Zhu, J.-H.; Wang, H.-D.; Liang, Y.-J. Control of Pore Size and Permeability of a Glucose-Responsive Gating Membrane for Insulin Delivery. *J. Controlled Release* **2004**, *97* (1), 43−53.

(26) Cai, T.; Neoh, K.; Kang, E.; Teo, S. Surface-Functionalized and Surface-Functionalizable Poly (vinylidene fluoride) Graft Copolymer Membranes via Click Chemistry and Atom Transfer Radical Polymerization. *Langmuir* **2011**, *27* (6), 2936−2945.

(27) Ulbricht, M.; Belfort, G. Surface Modification of Ultrafiltration Membranes by Low Temperature Plasma II. Graft Polymerization onto Polyacrylonitrile and Polysulfone. *J. Membr. Sci.* **1996**, *111* (2), 193−215.

(28) Chenette, H.; Robinson, J. R.; Hobley, E.; Husson, S. M. Development of High-Productivity, Strong Cation-Exchange Adsorbers for Protein Capture by Graft Polymerization from Membranes with Different Pore Sizes. *J. Membr. Sci.* **2012**, *423*, 43−52.

(29) Bhattacharjee, S.; Dong, J.; Ma, Y.; Hovde, S.; Geiger, J. H.; Baker, G. L.; Bruening, M. L. Formation of High-Capacity Protein-Adsorbing Membranes Through Simple Adsorption of Poly (acrylic acid)-Containing Films at Low pH. *Langmuir* **2012**, *28* (17), 6885−6892.

(30) Kim, D.; Tzeng, P.; Barnett, K. J.; Yang, Y. H.; Wilhite, B. A.; Grunlan, J. C. Highly Size-Selective Ionically Crosslinked Multilayer Polymer Films for Light Gas Separation. *Adv. Mater.* **2014**, *26* (5), 746−751.

(31) Bhattacharya, A.; Misra, B. Grafting: A Versatile Means to Modify Polymers: Techniques, Factors and Applications. *Prog. Polym. Sci.* **2004**, *29* (8), 767−814.

DOI: 10.1021/acsami.5b05592
ACS Appl. Mater. Interfaces 2015, 7, 19746−19754

(32) Morones-Ramírez, J. R. Coupling Metallic Nanostructures to Thermally Responsive Polymers Allows the Development of Intelligent Responsive Membranes. *Int. J. Polym. Sci.* **2014**, *2014*, 1−7.
(33) Hautojärvi, J.; Kontturi, K.; Näsman, J. H.; Svarfvar, B. L.; Viinikka, P.; Vuoristo, M. Characterization of Graft-Modified Porous Polymer Membranes. *Ind. Eng. Chem. Res.* **1996**, *35* (2), 450−457.
(34) Bates, F. S.; Hillmyer, M. A.; Lodge, T. P.; Bates, C. M.; Delaney, K. T.; Fredrickson, G. H. Multiblock Polymers: Panacea or Pandora's Box? *Science* **2012**, *336* (6080), 434−440.
(35) Seo, M.; Hillmyer, M. A. Reticulated Nanoporous Polymers by Controlled Polymerization-Induced Microphase Separation. *Science* **2012**, *336* (6087), 1422−1425.
(36) Akthakul, A.; Salinaro, R. F.; Mayes, A. M. Antifouling Polymer Membranes with Subnanometer Size Selectivity. *Macromolecules* **2004**, *37* (20), 7663−7668.
(37) Asatekin, A.; Olivetti, E. A.; Mayes, A. M. Fouling Resistant, High Flux Nanofiltration Membranes from Polyacrylonitrile-graft-poly (ethylene oxide). *J. Membr. Sci.* **2009**, *332* (1), 6−12.
(38) Barbey, R.; Klok, H.-A. Room Temperature, Aqueous Post-Polymerization Modification of Glycidyl Gethacrylate-Containing Polymer Brushes Prepared via Surface-Initiated Atom Transfer Radical Polymerization. *Langmuir* **2010**, *26* (23), 18219−18230.
(39) Barbey, R.; Laporte, V.; Alnabulsi, S.; Klok, H.-A. Postpolymerization Modification of Poly (glycidyl methacrylate) Brushes: An XPS Depth-Profiling Study. *Macromolecules* **2013**, *46* (15), 6151−6158.
(40) Kim, M.; Kiyohara, S.; Konishi, S.; Tsuneda, S.; Saito, K.; Sugo, T. Ring-Opening Reaction of Poly-GMA Chain Grafted onto a Porous Membrane. *J. Membr. Sci.* **1996**, *117* (1), 33−38.
(41) Saetia, K.; Schnorr, J. M.; Mannarino, M. M.; Kim, S. Y.; Rutledge, G. C.; Swager, T. M.; Hammond, P. T. Spray-Layer-by-Layer Carbon Nanotube/Electrospun Fiber Electrodes for Flexible Chemiresistive Sensor Applications. *Adv. Funct. Mater.* **2014**, *24* (4), 492−502.
(42) Martin, N. I.; Woodward, J. J.; Marletta, M. A. N G-Hydroxyguanidines from Primary Amines. *Org. Lett.* **2006**, *8* (18), 4035−4038.
(43) Loeb, S.; Sourirajan, S. *Saline Water Conversion-II*; Advances in Chemistry Series, 38; American Chemical Society: Washington, DC, 1963.
(44) Asatekin, A.; Kang, S.; Elimelech, M.; Mayes, A. M. Anti-Fouling Ultrafiltration Membranes Containing Polyacrylonitrile-graft-poly (ethylene oxide) Comb Copolymer Additives. *J. Membr. Sci.* **2007**, *298* (1), 136−146.
(45) Read, B. Mechanical Relaxation in Some Oxide Polymers. *Polymer* **1962**, *3*, 529−542.
(46) Kenyon, A.; Rayford, M. Mechanical Relaxation Processes in Polyacrylonitrile Polymers and Copolymers. *J. Appl. Polym. Sci.* **1979**, *23* (3), 717−725.
(47) Smolders, C.; Reuvers, A.; Boom, R.; Wienk, I. Microstructures in Phase-inversion Membranes. Part 1. Formation of Macrovoids. *J. Membr. Sci.* **1992**, *73* (2), 259−275.
(48) Peng, N.; Widjojo, N.; Sukitpaneenit, P.; Teoh, M. M.; Lipscomb, G. G.; Chung, T.-S.; Lai, J.-Y. Evolution of Polymeric Hollow Fibers as Sustainable Technologies: Past, Present, and Future. *Prog. Polym. Sci.* **2012**, *37* (10), 1401−1424.
(49) Faraone, A.; Magazu, S.; Maisano, G.; Migliardo, P.; Tettamanti, E.; Villari, V. The Puzzle of Poly (ethylene oxide) Aggregation in Water: Experimental Findings. *J. Chem. Phys.* **1999**, *110* (3), 1801−1806.
(50) Meireles, M.; Bessieres, A.; Rogissart, I.; Aimar, P.; Sanchez, V. An Appropriate Molecular Size Parameter for Porous Membranes Calibration. *J. Membr. Sci.* **1995**, *103* (1), 105−115.
(51) Sanchez, S. A.; Gratton, E.; Zanocco, A. L.; Lemp, E.; Gunther, G. Sucrose Monoester Micelles Size Determined by Fluorescence Correlation Spectroscopy (FCS). *PLoS One* **2011**, *6* (12), 29278−29283.
(52) Su, B.; Wang, T.; Wang, Z.; Gao, X.; Gao, C. Preparation and Performance of Dynamic Layer-by-Layer PDADMAC/PSS Nanofiltration Membrane. *J. Membr. Sci.* **2012**, *423*, 324−331.
(53) Schauer, J.; Kobayashi, T. Salt Separation by Charged Membranes. *Collect. Czech. Chem. Commun.* **1994**, *59* (6), 1356−1360.
(54) Fornasiero, F.; Park, H. G.; Holt, J. K.; Stadermann, M.; Grigoropoulos, C. P.; Noy, A.; Bakajin, O. Ion Exclusion by Sub-2-nm Carbon Nanotube Pores. *Proc. Natl. Acad. Sci. U. S. A.* **2008**, *105* (45), 17250−17255.
(55) Nightingale, E., Jr Phenomenological Theory of Ion Solvation. Effective Radii of Hydrated ions. *J. Phys. Chem.* **1959**, *63* (9), 1381−1387.
(56) Schaep, J.; Van der Bruggen, B.; Vandecasteele, C.; Wilms, D. Influence of Ion Size and Charge in Nanofiltration. *Sep. Purif. Technol.* **1998**, *14* (1), 155−162.
(57) Wang, X.-L.; Tsuru, T.; Nakao, S.-i.; Kimura, S. The Electrostatic and Steric-Hindrance Model for the Transport of Charged Solutes Through Nanofiltration Membranes. *J. Membr. Sci.* **1997**, *135* (1), 19−32.
(58) Donnan, F. G. The Theory of Membrane Equilibria. *Chem. Rev.* **1924**, *1* (1), 73−90.
(59) Schaep, J.; Vandecasteele, C.; Wahab Mohammad, A.; Richard Bowen, W. Modelling the Retention of Ionic Components for Different Nanofiltration Membranes. *Sep. Purif. Technol.* **2001**, *22*, 169−179.
(60) Wade Jr, L. *Organic-Chemistry*, 8th ed.; Pearson Prentice Hall: Upper Saddle River, NJ, 2012.
(61) Verissimo, S.; Peinemann, K.-V.; Bordado, J. Influence of the Diamine Structure on the Nanofiltration Performance, Surface Morphology and Surface Charge of the Composite Polyamide Membranes. *J. Membr. Sci.* **2006**, *279* (1), 266−275.
(62) Saeki, S.; Kuwahara, N.; Nakata, M.; Kaneko, M. Phase Separation of Poly(ethylene glycol)- Water-Salt Systems. *Polymer* **1977**, *18* (10), 1027−1031.
(63) Kohonen, M. M.; Karaman, M. E.; Pashley, R. M. Debye Length in Multivalent Electrolyte Solutions. *Langmuir* **2000**, *16* (13), 5749−5753.

DOI: 10.1021/acsami.5b05592
ACS Appl. Mater. Interfaces 2015, 7, 19746−19754